

Comparative study of the mechanism
underlying orientation selectivity in mammals

Yamni Mohan

Contents

1 Acknowledgements	4
2 Abstract	5
3 Introduction	6
4 Literature Review	7
4.1 Cross-species comparison	7
4.1.1 Laminar Organisation of neuronal responses.	8
4.1.2 Orientation selectivity	11
4.2 Sub-cortical orientation biases	13
4.2.1 Radial Bias in the cortex	13
4.2.2 Orientation biases in the superior colliculus	13
4.3 Effect of Inhibition	13
4.4 Spatial Frequency Tuning	13
4.5 Spatial Frequency dependence of Orientation Tuning	13
4.6 Superior Colliculus	13

4.6.1	Anatomy and projections of the superior colliculus	15
4.6.2	Response properties of the superior colliculus	15
4.6.3	Direction Selectivity	15
4.7	Literature Review/ Background	16
4.7.1	The mammalian primary visual cortex	16
4.7.2	Mechanisms of orientation selectivity	19
4.7.3	Functional organisation of V1	23
5	Methods	27
5.1	Surgery and Anaesthesia	27
5.2	Stimulus Presentation	28
5.2.1	Stimulus used for experiment one	28
5.2.2	Bar stimuli	29
5.2.3	Grating stimuli	29
5.3	Electrophysiology	30
5.4	Optical Imaging of Intrinsic Signals	30
5.5	Iontophoresis	31
5.6	Histology	32
5.6.1	Cresyl Violet Staining	33
5.6.2	Track Reconstruction	33
5.7	Data Analysis	34
5.7.1	Post- stimulus time histograms	34
5.7.2	Defining response	34

5.7.3	Measures of orientation tuning	35
5.7.4	Spatial Frequency Tuning	35
6	Where do orientation biases come from?	36
6.1	Abstract	37
6.2	Introduction	38
6.3	Methods	40
6.3.1	Electrophysiology	40
6.3.2	Stimuli	41
6.3.3	Data Analysis	41
6.4	Results	42
6.4.1	Anatomical location of units	42
6.4.2	Orientation Selectivity	43
6.4.3	Spatial Frequency Tuning	45
6.5	Discussion	47
6.5.1	Anatomical Relevance	48
6.5.2	Orientation selectivity in shrew superior colliculus . . .	48
6.5.3	Direction selectivity	48
6.5.4	Similarities and differences with other species	48
7	Orientation anisotropies in the inputs to the primary visual cortex of macaques	49
7.1	Abstract	50
7.2	Introduction	51

7.3	Methods	51
7.3.1	Data Collection	51
7.3.2	Analysis	53
7.4	Results	58
7.5	Discussion	60
7.6	Conclusions	60
8	Issues to be solved	61

Chapter 1

Acknowledgements

Chapter 2

Abstract

Chapter 3

Introduction

Chapter 4

Literature Review

4.1 Cross-species comparison

In my thesis, I am going to compare the laminar organisation of the primary visual cortex, response properties of neurons observed here and focus on the mechanisms involved in the generation of orientation selectivity. Most vision experiments are conducted on cats. But there is a line of evidence which suggests that the way in which orientation selectivity evolves is different between carnivores and primates. In particular, there is a break in the mouse visual cortex where orientation selectivity is organised in a salt and pepper fashion rather than the usual columnar organisation observed in other species. Here we compare the mechanism of orientation selectivity in three different species, namely cats, tree shrews and macaques.

4.1.1 Laminar Organisation of neuronal responses.

Scope of the section: In my thesis I am going to concentrate mainly on feedforward pathways. In the visual system, information from the eyes is transmitted from the retina to the lateral geniculate nucleus (LGN). The LGN then transmits information to the primary visual cortex (V1). V1 consists of six layers. LGN input to V1 terminates in layer 4 which then provides input to layer 2/3 of the cortex which in turn provides input to higher visual areas. There is internal feedback from horizontal networks within areas which will be examined here. Feedback also comes to V1 from the extrastriate areas and V1 itself provides feedback to LGN these are not examined in great detail here. The feedforward pathway is highly conserved but there are certain species specific differences in the responses of neurons in these lamina. The similarities and differences are highlighted below. See figure 1 for a summary of the laminar organisation. I am also going to examine the distribution of orientation and spatial frequency information in these layers.

An image of cat V1 with the layers marked is shown in figure 2.

Laminar organisation of neuronal responses in cats area 17

As detailed above, in the cat, LGN inputs terminate at layer 4 of V1. Additionally, LGN also projects to area 18 in the cats. Within layer 4, the C lamina projects to the top and bottom of layer 4 while the A laminae projected throughout layer 4 and to the bottom of layer 3. The C lamina projections

essentially "bracket" the A laminae projections (LeVay and Gilbert, 1976). This layer is not as prominent in cats as in other species. Neurons are classified into X or Y type based on the linearity of their response. X cells project to layer 4C and Y cells in layer 4ab (Gilbert and Wiesel, 1979). Lamina A and C= X- input and lamina A1= y input. Lamina B seems to have a lack of x-activity and presence of w-activity.

Laminar organisation of neuronal responses in macaques primary visual cortex

In macaques, the laminar organisation is yet again slightly different. Inputs to the cortex are organised in layer 4 but there is now the added complexity colour information.

Laminar organisation of neuronal responses in tree shrew primary visual cortex

As in cats and macaques, geniculate inputs terminate in layer 4 of the tree shrew cortex (figure 2c). Unlike cats and macaques however, this laminar segregation is between on and off neurons. Layer 4 is further sub-divided into layer 4a and 4b. Layer 4a receives input from the on laminae of the tree shrew LGN and the layer 4b receives input from off laminae of the LGN. There is a 'cleft' segregating the sub-layers on either side of which are present neurons that are tuned to both on and off stimuli. The neurons are also segregated on the basis of ocularity. Neurons that receive contralateral

input are found along the outer edges of layer 4, sandwiching neurons that receive binocular inputs. Anatomically, it has been shown that there are parallel inputs from layer 4 to layer 2/3. Inputs from the outer edges of layer 4 are said to project to the lower part of layer 2/3, inputs from the middle of layers 4a and 4b to the middle of layer 2/3 and inputs from the bottom layer of layer 4a and top layer of layer 4b to the topmost layer of layer 2/3.

Neurons in layer 4 of tree shrews behave rather differently when compared to layer 4 of cats. As mentioned earlier, they are segregated based on their polarity (whether they are on centred or off centred). Further, they also exhibit properties similar to their LGN counterparts in cats. For example, they are broadly tuned to orientation and show a low-pass spatial frequency tuning. Van Hooser et al., 2013 showed that layer 4 neurons in tree shrews are slightly more tuned to orientation than LGN neurons in tree shrew and apart from an attenuation of response to higher temporal frequencies, resemble LGN neurons quite closely. The sharper orientation tuning has been particularly attributed to the edges of layer 4, namely the top of layer 4a and the bottom of layer 4b. Layer 4 neurons are reported as having a similar spatial frequency tuning curve to lgn neurons. Layer 2/3 neurons in tree shrews are however as sharply tuned to both orientation and spatial frequency as the layer 2/3 neurons in cats and monkeys; ie., there are neurons sharply tuned for orientation and organised in columns and the spatial frequency is band pass tuned at the optimum orientation.

Anatomically, Fitzpatrick and colleagues suggest that the edges of layer

4 project to the bottom of layer 2/3. However, physiologically, this indicates a connection between a region sharply tuned for orientation to a region that shows orientation selectivity to a lesser extent. This drop in orientation selectivity has been observed between simple and complex cells. Further, other anatomical sources suggest that, similar to the cats and macaques, lgn inputs terminate in the lower parts of layer 2/3.

4.1.2 Orientation selectivity

The origin of sharp orientation selectivity as observed in the primary visual cortex has long been debated. Hubel and Wiesel when they first described it proposed a model by which this sharp orientation tuning could arise. They suggested that circular LGN receptive fields which are arranged in a row provide input to a cortical neurons which is then tuned to an orientation parallel to that of the LGN receptive fields. This model falls short on multiple accounts. For example it cannot account for such properties as the contrast insensitivity of orientation tuning. It also does not account for the presence of large amounts of inhibition in the primary visual cortex. Finally, it has been demonstrated that neurons in sub cortical areas are already tuned for orientation and Hubel and Wiesel's model does not account for this.

One model that takes these into account involves sharpening of the orientation biases observed in the V1. In this model, LGN inputs that are already biased for orientation are further sharpened by intra-cortical mechanisms such as orientation non-specific inhibition. This model not only accounts for

orientation selectivity but also spatial frequency tuning responses observed.

In cats, LGN neurons show a broad orientation bias and also demonstrate a low pass spatial frequency tuning. Layer 4 neurons on the other hand are sharply tuned to orientation and show a band pass orientation tuning. In the LGN, at the optimum spatial frequency, the neurons are broadly tuned to orientation. At higher spatial frequencies they are sharply tuned to orientation almost to the extent observed in V1. Cortical neurons receive direct excitatory inputs from the geniculate. They also receive di-synaptic inhibitory input through an inhibitory interneuron. The cortical neuron receives excitatory input that is biased for a certain orientation from the LGN. At the same time, it also gets inhibitory inputs that are either tuned to an orthogonal orientation or broadly tuned to orientation. Then at lower spatial frequencies where none of the geniculate neurons are sharply tuned for orientation, both the excitatory and the inhibitory inputs cancel each other out. But at higher spatial frequencies, the orientation perpendicular to the direction of the inhibition gets no suppression. As a result, the cortical neuron now fires for this orientation.

This mechanism would explain both sharp orientation tuning and spatial frequency tuning of the neuron.

4.2 Sub-cortical orientation biases

4.2.1 Radial Bias in the cortex

This will lead to experimental chapter 1

4.2.2 Orientation biases in the superior colliculus

This will lead to experimental chapter 2

4.3 Effect of Inhibition

This will lead to experimental chapter 3 and 4.

4.4 Spatial Frequency Tuning

4.5 Spatial Frequency dependence of Orientation Tuning

4.6 Superior Colliculus

The superior colliculus plays an important role in visual processing in the tree shrews. It has two functional sub-divisions, the superficial layers which are involved in form perceptions and the deeper layers which are involved in head movement. The superficial layers receive retinal inputs and projects to

extrastriate visual cortex via the pulvinar. They also provide input to other visual areas of the thalamus like the LGN. The visual pathway through the superior colliculus to the temporal cortical region is said to be an alternate to the geniculostriate pathway. If this were indeed the case, then SC could be the dLGN equivalent in this alternate pathway. This would mean that features important in form perception such as orientation selectivity would need to be conveyed to the temporal regions. The orientation input could be derived from striate cortical neurons which are said to generate orientation tuning de novo. However, in studies where V1 was removed, form perception was preserved in animals. This suggests that the basis of orientation selectivity is probably sub-cortical. Infact, orientation biases have been reported in structures as early along the visual pathway as the retina. Cat and macaque retinal ganglion cells are tuned to orientation at higher spatial frequencies. These biases can then be sharpened using intracortical mechanisms.

The superior colliculus also known as the tectum in non-mammalian species is a midbrain nucleus that plays an important role in vi is different in different organisms. Broadly it is divided into two functional areas. The dorsal layers of the SC play an important role in form perception. The lower layers are involved in an animal's orienting behaviour.

4.6.1 Anatomy and projections of the superior colliculus

4.6.2 Response properties of the superior colliculus

In cats, neurons in the superficial layers of the superior colliculus are selective to direction of a stimulus. In particular, cells respond best to the direction away from the vertical meridian. SC neurons in other species(eg: frogs) lack this specificity while maintaining the direction selectivity. Other animals like primates seem to entirely lack direction selectivity in the superior colliculus. Orientation selectivity in the superficial layers of the superior colliculus has not been reported in most species. However, a number of recent papers suggest that smaller mammals such as mice demonstrate orientation selectivity in the superficial layers. Studies of orientation selectivity in the superficial layers of the tree shrew have shown that a small proportion of neurons in the superficial layers are selective to orientation. This study also does not comment on the direction selectivity of neurons in the superficial SC. Direction selectivity is a rare trait in the tree shrew visual system with only a small portion of cells even in the striate cortex demonstrating this property.

4.6.3 Direction Selectivity

29% of cells in macaque V1 are direction selective 71% not (Ratio of opt to non-opt > 0.5= non directional; DeValois et al., 1981)

4.7 Literature Review/ Background

4.7.1 The mammalian primary visual cortex

The primary visual cortex (V1 or Area 17) has been studied extensively. Its organising features such as the functional specialisation of individual layers and its columnar architecture have been hailed as representative of the organisation of other sensory cortices. Briefly, feed-forward geniculate (LGN) inputs to V1 terminate in layer 4 and 6. Layer 4 neurons project to the superficial cortical layers (layers 2 and 3) from which extrastriate projections originate. Infragranular layers are believed to be the origins of feedback to the subcortical visual areas (see Douglas & Martin, 2004 for review). Within this canonical framework, the functional nature of inputs vary. In most species, visual information is segregated on the basis of their functional properties into different pathways. In cats, macaques and tree shrews, the functional segregation differs. These differences are briefly examined below (also see Figure 1 for summary). In macaques, chromatic and achromatic information is segregated in different pathways in their projections from retina to LGN to V1. The magnocellular pathway (M-) transmits achromatic information and the neurons in this pathway respond to luminance changes (Hicks et al., 1983; Kaplan et al., 1990; Dacey, 2001). The parvocellular (P-) (Hicks et al., 1983; Kaplan et al., 1990; Merigan & Maunsell, 1993) and koniocellular (K-) (Dacey, 2001; Roy et al., 2009) pathways transmit chromatic information. The major targets of these projections in macaques are in layer 4C, 4C and layer 3B of

V1 (Casagrande & Kaas, 1994). This segregation was believed to be maintained even in extrastriate areas (Bullier & Henry, 1980; Casagrande & Kaas, 1994). However, there is evidence to suggest that there is considerable overlap in inputs as early as layer 4 (Casagrande & Kaas, 1994; Callaway, 1998; Vidyasagar et al., 2002). In comparison, LGN inputs to V1 in the tree shrew are segregated into ON, OFF and W-cell pathways (Conway & Schiller, 1983; Conley et al., 1984; Holdefer & Norton, 1995). ON cells respond to increases in luminance and OFF cells respond to decreases in luminance. The ON, OFF and W-cells terminate in layers 4A, 4B and 3C of V1 respectively (Conley et al., 1984). Layer 4A mostly have on neurons and 4B, mostly off neurons (for review, see Fitzpatrick, 1996). In cats, the inputs to V1 segregate differently. X and Y cells of the LGN project to layers 4C and 4A+B respectively (Wilson et al., 1976; LeVay & Gilbert, 1976). X-cells show a sustained response when presented a stimulus. They also sum signals linearly within their receptive fields. That is, when presented with dark and light stimulus regions over the receptive field at the appropriate phase, there is virtually no response as the cell sums the signals from the ON and OFF sub-regions linearly. Y cells on the other hand sum non-linearly within their receptive fields and they also have a transient response when a stimulus is presented, irrespective of phase (Enroth-Cugell & Robson., 1966). While there are major differences in physiological properties of the different pathways, some similarities have been found. For example, it has been shown that there is some extent of on/off segregation as observed in the tree shrew within the parvocellular

layers of the macaque LGN (Schiller & Malpeli, 1978). It was also originally thought that parvocellular cells were X-cells and magnocellular cells were Y-cells (Dreher et al., 1976). However, this is not entirely the case. While most P-cells are indeed X cells, 75% of M- cells are also X-cells in macaques (Shapley et al., 1981). Similarly, most neurons in the tree shrew LGN are also X cells, with cells showing non-linear summation only observed in 2 of the 6 layers (Conway & Schiller, 1983). Despite the differences highlighted above, the supragranular layers have similar functional architecture in all three species. Hubel and Wiesel (1962; 1968) first demonstrated the presence of orientation columns in cats and in macaques using electrophysiology. This was also later demonstrated using autoradiographic studies (Hubel et al., 1978). Optical imaging of intrinsic signals showed that orientation in the V1 was organised in columns which converged at pinwheel centres in cats and macaques (Bonhoeffer & Grinvald, 1991; Bartfeld & Grinvald, 1992). In the tree shrews, Humphrey and Norton (1980) suggested that orientation columns were organised in elongated columns perpendicular to the V1/V2 border. However, later Bosking et al. (1997) showed using optical imaging of intrinsic signals that orientation columns were organised in a similar fashion to what was observed in macaques and cats. Given this, it may be supposed that while the inputs to V1 in cats, macaques and tree shrew are different, the mechanism through which orientation tuning develops in all three species maybe similar.

4.7.2 Mechanisms of orientation selectivity

Cortical units selectively respond to edges of a narrow range of orientations unlike their LGN counterparts which respond to almost all orientations. Initial insights into this orientation selectivity, were gained from experiments conducted by Hubel and Wiesel. They proposed a theory of excitatory convergence to explain the sharp orientation tuning they observed in cortical simple cells in cats (Hubel & Wiesel, 1962) and macaques (Hubel & Wiesel, 1968). They suggested that un-oriented, spatially offset LGN receptive fields arranged collinearly along the long axis of the cortical receptive field, provided inputs to a simple cell giving rise to the classical, elongated receptive fields and sharp orientation tuning observed in cats and macaques (Hubel & Wiesel, 1962; 1968). While this has been the most prominent theory of orientation selectivity, still retaining support some 50 years after its conception, it is not without its flaws(for review see Vidyasagar et al., 1996; Ferster & Miller, 2000). For example, while it explains length summation in the cortical neurons, the excitatory convergence model is unable to account for the contrast invariance observed in simple cells (Ferster & Miller, 2000; Carandini, 2007). The effect of inhibition generated by intracortical interactions have also been implicated in generating the sharp orientation tuning (Creutzfeldt et al., 1974; Sillito, 1975; 1979; Tsumoto et al., 1979; Sillito et al., 1980). In the light of these short comings, many alternative models of orientation selectivity have been proposed. Other models of orientation tuning involve the role of intracortical circuits in the generation of sharp orientation tuning. These

models include processes such as cross-orientation inhibition generated by inhibitory interneurons (Creutzfeldt et al., 1974), iso-orientation facilitation (Douglas et al., 1991; Volgushev et al., 1995), spatially offset excitatory and inhibitory inputs (Heggenlund, 1981) and excitatory inputs originating from on and off centred neurons (Soodak, 1987). The models that implicate the intracortical circuits also do not take into account of the weak orientation bias reported in the LGN afferents to the cortical cell. The studies that have shown orientation biases in the afferent input to the cortical cell had assumed that this bias originates from a Hubel and Wiesel type excitatory convergence (for example, see Ferster & Miller, 2000). Soodak's (1987) model ignores the evidence that in studies where APB (suppresses ON responses in bipolar cells) is administered intravitreally in cats, the orientation tuning of the remaining OFF response often stays unchanged in both cats and monkeys (Schiller, 1982, 1986; Sherk & Horton, 1984; for review see Schiller, 1992). One model of orientation selectivity suggests that the initial orientation tuning is inherited from the orientation biases of LGN neurons (Vidyasagar et al., 1996). According to this model, the bias in the afferent LGN input to a striate simple cell is established by the excitatory input from one or more LGN receptive fields broadly tuned to the same orientation. In line with this model, orientation biases have been demonstrated in the LGN of cats (Vidyasagar & Urbas, 1982), macaques (Shou & Leventhal, 1989) and tree shrews (Van Hooser et al., 2013). Once an initial orientation selectivity is established from the LGN input, recurrent excitation and inhibition caused by the extensive

horizontal connections in V1; cross-orientation inhibition and non-specific inhibition may all contribute to sharpen orientation tuning (Vidyasagar et al., 1996). Inhibition has been shown to play an important role in establishing the sharp orientation tuning observed in cat visual cortex. It was shown that each layer 4 simple cell received monosynaptic excitatory input as well as a disynaptic inhibitory input in the cat (Creutzfeldt & Ito, 1968; Ferster & Lindstrom, 1983). Intracellular recordings from V1 neurons where a stimulus moving over the excitatory receptive field often elicited inhibitory post synaptic potentials (IPSP; Creutzfeldt et al., 1974) suggesting that inhibition played an important role in sharpening orientation selectivity. When bicuculline, a GABA_A receptor antagonist was applied to V1, a significant reduction in the orientation tuning of several cells was found with orientation tuning abolished entirely in some neurons (Sillito, 1979). In a later study, Sillito et al. (1980) used a more potent GABA antagonist N-methyl bicuculline and found that 9 out of 13 simple cells showed complete loss of orientation selectivity. This mechanism by which the broadly tuned excitatory inputs are sharpened by means of disynaptic inhibition could also explain other cortical properties such as spatial frequency tuning (Vidyasagar & Heide, 1984; Vidyasagar & Mueller, 1984; Vidyasagar, 1987) and cortical length response functions (Vidyasagar, 1987; Kuhmann & Vidyasagar, 2011). Sine-wave gratings have been used to study both spatial frequency tuning and orientation tuning in neurons along the visual pathway. When thus examined, cortical cells exhibit band-pass tuning to spatial frequency i.e., they respond to a

narrow range of spatial frequencies. Their LGN counterparts on the other hand show a low-pass spatial frequency tuning (Maffei & Fiorentini, 1973; DeValois et al., 1980; Van Hooser et al., 2013). Further, orientation tuning of neurons are dependent on the spatial frequency of the stimulus used. At lower spatial frequencies, retinal and LGN neurons respond well to gratings of all orientations. At higher spatial frequencies, on the other hand, the orientation selectivity sharpen markedly; i.e., at the non-optimum orientation there is less response to a stimulus when compared to the optimum orientation (Levick & Thibos, 1980; 1982; Vidyasagar & Heide, 1984). As LGN neurons do not show orientation specificity at lower spatial frequencies, if these were to drive the cortical inhibitory neurons, the response of cortical neuron studied will be attenuated at lower spatial frequencies through orientation non-specific inhibition. At higher spatial frequencies, the excitatory input that the cortical cells receive from the LGN will be tuned to orientation (Vidyasagar & Heide, 1984; Vidyasagar, 1987; Kuhlmann & Vidyasagar, 2011). It was originally proposed in the tree shrews that sharp orientation selectivity of layer 2/3 neurons arose from Hubel and Wiesel (1962) style excitatory convergence of feedforward inputs from layer 4 (Chisum et al., 2003; Mooser et al., 2004) with inhibition exerted by the extensive horizontal interactions leading to further sharpening (as suggested by Ferster & Miller, 2000). In a recent study by Huang et al (2014), it was shown that the neurons belonging to a particular orientation domain summed their inputs linearly when domains of similar orientation were optogenetically stimulated, questioning the role

of inhibition in generating sharp orientation selectivity. However, it must be noted that their optogenetic stimulation would not have activated GABAergic neurons in the cortex and any excitation of inhibitory neurons would be post-synaptic which may not have been sufficient to alter the response (Huang et al., 2014). As a result, the role of inhibition in sharpening orientation selectivity in the tree shrew cortex has thus far remained unresolved. Layer 4 neurons in tree shrews show broad orientation bias and low pass spatial frequency tuning responses similar to their LGN counterparts (Chisum et al., 2003; Van Hooser et al., 2013; Scholl et al., 2013). There are extensive short and long range horizontal connections within the tree shrew layer 2/3 which contribute to the orientation response of their target neurons (Bosking et al., 1997; Chisum et al., 2003). Based on this evidence, it may be hypothesised that in tree shrews, sharp orientation tuning observed in the layer 2/3 neurons comes about by the sharpening of orientation biases of the layer 4 neurons through orientation non-specific inhibition similar to the transition from LGN to layer 4 simple cell suggested in cats (Vidyasagar, 1987; Vidyasagar et al., 1996). Experiments 1 and 2 will be conducted to test this hypothesis.

4.7.3 Functional organisation of V1

One of the striking features of the primary visual cortex in mammals is the organisation of features such as orientation selectivity and the eye of origin into functional modules (Hubel and Wiesel, 1962; 1968). The organisation of

orientation selectivity is such that neurons that have similar orientation preferences are clustered together to form orientation columns (Hubel & Wiesel, 1962; 1968) with different orientation domains appearing to converge on to pinwheel centres (Bonhoeffer and Grinvald, 1991). In the macaque, it has been suggested that the presence of these modules may not be merely functional but rather that there may be a physiological substrate in the cytochrome oxidase (CO) blobs (Livingstone and Hubel, 1982). In the primary visual cortex, there are regularly spaced regions of the cortex which stain darkly for the metabolic enzyme, cytochrome oxidase. Termed cytochrome oxidase blobs (CO blobs), these regions indicate areas of high metabolic activity. Layer 4, where subcortical inputs to V1 terminate- hence increasing the metabolic needs of this region, also stains darkly for cytochrome oxidase (Wong-Riley, 1979; Livingstone & Hubel, 1982). In layer 2/3 of the macaque, cytochrome oxidase blobs are evenly distributed and coincide with the centres of ocular dominance columns as identified by 2-deoxyglucose studies (2 DG). In 2DG studies however, the orientation columns showed up as a mosaic rather than as distinct rows of blobs (Hubel & Horton, 1981). Optical imaging studies on the other hand suggested that the orientation pinwheels often avoided the centres of the ocular dominance columns but did not necessarily coincide with centres of the CO blobs suggesting that these two systems co-exist independently (Bartfeld and Grinvald, 1992). It is however, possible that the orientation columns and CO blobs have a more complicated relationship. It has also been shown that CO blobs are co-localised with regions

of layer 3B which receive LGN input (Livingstone & Hubel, 1982). It could be that CO blobs coincide with the location of of the broadly tuned thalamic inputs to the cortex. In the cortex, ocular dominance inputs, orientation selective inputs and ON/OFF inputs are segregated in columns (Hubel & Wiesel, 1962; 1968; Jin et al., 2008, 2011). These columns however, are not separate but partially overlap, as has been described earlier. It has recently been proposed that LGN afferents broadly tuned for all three properties terminate in separate modules in the cortex and the interactions between these could give rise to all the other orientations, ocular dominance (from 1-7) and subfields with different ON and OFF strengths. For example, an ON afferent from the right eye tuned to vertical orientation and an ON afferent from the right eye tuned to horizontal orientation will terminate separately and give rise to all the other orientations in between them (Vidyasagar & Eysel, 2015, TINS invited review).

If the orientation tuning of V1 neurons comes about due to the sharpening of subcortical orientation biases, then in order to not lose resolution, orientation information should be coded in a limited number of broadly tuned channels in the retina, similar to what has been observed in colour (Vidyasagar, 1987). Orientation asymmetries have previously been shown in the retina (in cat, Levick & Thibos, 1982), in the LGN (Shou & Leventhal, 1989; Vidyasagar & Urbas, 1989), in the cortex (Chapman & Bonhoeffer, 1998) and at a behavioural level in humans (for example see Orban et al., 1984). Of these, radial orientation bias has in the recent years gained more

support than the oblique effect(Sasaki et al., 2006; Swisher et al., 2010). Radial orientation' is the angle theline joining the centre of the receptive field and the foveal centre subtends to the horizontal. While generating orientation maps (as in fig 2C) from optical imaging of intrinsic signals, the response to each individual condition is first high-pass filtered and then low-pass filtered. When the low pas filter was omitted, it was found that the signal (believed to be pre-synaptic in nature) was tuned to the radial orientation (Vidyasagar et al., 2014). The maps thus obtained were termed 'veridical maps'. In figure 2 the veridical orientation maps that have been obtained in our lab are presented. In all the maps generated thus far, the left operculum of macaque V1 was imaged and as a result, the same part of the receptive field was imaged (radial angle corresponding to the second quadrant- between 90 $^{\circ}$ and 180 $^{\circ}$). In the veridical orientation maps that have been presented, there are also patches (indicated by the black arrows). The relationship between these patches, cytochrome oxidase blobs and the orientation columns observed in the filtered maps will be examined in experiment 3.

Chapter 5

Methods

5.1 Surgery and Anaesthesia

All experiments have ethics approval. This study looked at cortical responses to visual stimuli in three different species, cats, macaques and tree shrews. This chapter outlines the methodology that was common in all three animals. Experiment specific methodology is incorporated in the individual chapters.

In all animals, initial anaesthesia was induced using a mixture of ketamine and xylazine (Varied dosage). Once the animals were anaesthetised, tracheostomy and venous cannulation (cephalic in cats and macaques; femoral in tree shrews) was completed. During the experiment, anaesthesia was maintained using a gaseous mixture containing nitrogen, oxygen and carbon-dioxide (See table for dosage). Paralysis was established using an intravenous bolus of norcuron and was maintained using vecuronium administered in-

travenously. The animal's body temperature was maintained between 36-37 degrees using a servo controlled heating blanket. ECG and EEG were monitored throughout the experiment and the level of anaesthesia was adjusted accordingly. Following initial surgery, a craniotomy and durotomy were conducted over the location of the primary visual cortex (V1, see table for horsley-clarke co-ordinates.). Once recordings were completed, the experiment was terminated by administering the animal an overdose of pentobarbitone (dosage) intravenously. The animal was then perfused intracardially using phosphate buffer, a paraformaldehyde solution; the brain was removed and stored in a solution of 25 percent sucrose for cryoprotection. The brain was later processed for histology.

5.2 Stimulus Presentation

Stimulus was presented on a barco monitor (Frame rate= 80 Hz). All stimulus was generated in SDL and presented using ViSaGe stimulus generator. For the first experimental chapter, we used full field square wave gratings. For the rest of the experimental chapters, we used bars and smaller, sinusoidal gratings.

5.2.1 Stimulus used for experiment one

For the first experimental chapter, 'Radial bias in the inputs to the cortex', the anaesthetised animal was presented full-field, square wave gratings with

SF= between 1 and 4 cpd. The temporal frequency was 2.2 Hz and contrast was set at 100 percent. The stimulus was presented for 7.3s followed by an interstimulus interval of 10s. The gratings that were presented were of different orientations between 0 and 157.5 degrees in 22.5 degree steps.

5.2.2 Bar stimuli

For all other experimental chapters, initially, a bar was presented to determine the orientation of a unit. As layer 2/3 neurons (in shrews; layer 4 in cats) were sharply tuned to orientation, they only responded to bars of certain orientations. For layer 4 neurons in shrews, thinner bars were used to determine orientation preference. The bars were also varied in length to account for length response functions, contrast and speed in order to optimise the stimuli and only study the effect of the dimension that was changed. During the experiment, optimum orientation was determined by looking at the peak responses of the orientation response obtained using a PSTHs.

5.2.3 Grating stimuli

Once the orientation of the stimulus was gauged, the animal was presented with grating stimuli to determine spatial frequency tuning of the neuron. To get spatial frequency tuning of the neurons, orientation, contrast, size of the grating were optimised and the spatial frequency was varied in 0.1 cpd steps (for tree shrews). This was repeated at four different orientations

45 degrees apart. The differences in the spatial frequency tuning between different orientations was examined.

5.3 Electrophysiology

Electrophysiological measurements were done using high impedance tungsten micro-electrodes (betn 4 and 18 megaohms.). The electrodes were inserted into the cortex and were plugged into a pre-amp. The signal from the pre-amp was passed through a antialiasing filter (high cut-off= 5000 Hz), a humbug was used to reduce 50 Hz line noise, and the resulting signal was passed through a band-pass filter (between 300 and 3000 kHz). The signal was digitised at 22.5 kHz using a analog to digital converter. The data was recorded using the spike 2 software. In order to ensure that our recordings were actually spiking outputs of neurons, we also made sure that we had a reasonable signal to noise ratio. A template of the spikes was built using spike 2 software and used for online analysis. The original signal was stored for later analysis.

5.4 Optical Imaging of Intrinsic Signals

Optical imaging of intrinsic signals was a technique established in the 1990s to look at the organisation of the cortex on a scale greater than the individual neuron level. It consists of fast-scanning ccd camera which has two lenses

attached face to face to it. This setup allows the user to specify a narrow depth of focus. The camera essentially looks at the changes in reflectance of the blood signal in response to a visual stimulus. It is based on the principle that the amount of oxygen present in the blood affects its reflectance. In response to neuronal activity, the amount of oxygenated haemoglobin in the blood decreases and the amount of deoxygenated haemoglobin in the blood increases. At certain wavelengths of light, this difference can be distinguished. At the isosbestic wavelength (570 microns), the reflectance of oxy and deoxy haemoglobin remains the same. At higher wavelengths, however, the difference in reflectance varies causing there to be change in signal. The reflectance of a region of cortex decreases in response to neural activity and this signal is captured in optical imaging. Accordingly, in response maps, activity is represented by dark patches.

5.5 Iontophoresis

Iontophoresis is a technique using which we can deliver small quantities of chemical intervention to neurons. For our experiments, we use a five barrel glass micropipette glued to a single barrel glass electrode (Tip diameters:; Average impedance:). In the technique, we eject small amounts of polarised current into the barrels containing the chemical intervention we wish to deliver. In order to delineate the effect due to drug intervention as against the ejection of current from the electrode, simultaneously a balance electrode

filled with an inert solution is used to eject current of the opposite polarity.

In this experiment, bicuculline is used to abolish inhibition. Bicuculine is a GABA A neurotransmitter blocker. GABA A is implicated in the transient response of neurons in V1. Getting rid of GABA A in the cortex will abolish the tuning of this transient response. GABA A blocking has shown to reduce the orientation tuning in some cases in the primary visual cortex. These studies were conducted using bars though. We are going to present gratings of different spatial frequencies and orientations to examine the effect of bicuculline in the primary visual cortex.

In this experimental set up, two of the five barrels are filled with Bicuculline, one with GABA which is used to test the effectiveness of bicuculine and one with Glutamate which is used to test the effectiveness of iontophoresis in general. One of the five micropipettes is filled with a saline solution. This is used as a balance. Our single barrel electrode is used as a recording electrode and is filled with pontamine blue. The recorded signal is processed as mentioned earlier. The pontamine blue is used to lesion the regions from which recordings were made for track reconstructions later.

5.6 Histology

After the experiment, the tissue was processed for histology as follows. The brain was stored in a 25 percent sucrose solution until it sank. This was to ensure that the tissue was cryoprotected. After this, the brain was blocked

so that only the areas of interest was processed. The brain was frozen in a cryostat and 50 micron sections were made. The sections were mounted on gelatinised slides. Once the sections were dry, they stained.

5.6.1 Cresyl Violet Staining

First the sections were dehydrated using increasing concentrations of ethanol. Then, chloroform was used to defatten the sections. This was followed by rehydrating sections in decreasing concentrations of ethanol. THe sections were then stained using Cresyl Violet Acetate solution (0.1 perc, Sigma) and differentiated using a solution of 5 percent acetic acid in 95 percent ethanol. It was then dehydrated using increasing concentrations of ethanol and fixed in histolene. The slides were then coverslipped.

5.6.2 Track Reconstruction

In order to reconstruct electrode tracks, we located the electrolytic lesions/ pontamine lesions that we made under the microscope and digitised those sections. The shrinkage was calculated by comparing the recorded and observed distances between lesions. This shrinkage calculation was used to calculate the actual depth of the units recorded. Based on the location of the unit, it was classified as layer 4 or layer 2/3 unit and this classification was used for further analysis.

5.7 Data Analysis

5.7.1 Post- stimulus time histograms

We have spikes based on a template. The response to a particular stimulus is arranged in a PSTH. The X-axis of a PSTH is time after stimulus has been presented and the Y-axis is the response (usually measured as spike counts or spike rates). The spikes that occur during stimulus presentation are binned in 20 ms bins and presented as a histogram and this is used for further analysis.

5.7.2 Defining response

When presented with a bar, response is the spike rate. Getting a maximum response just means getting maximum spike rate while a given stimulus crosses the receptive field. Whereas, this is not the same for gratings. A unit based on whether it demonstrates linear summation over its receptive field or not responds differently to a grating. For example, a simple cell gives a modulated response to a grating whereas a complex gives an unmodulated response. These response properties are so distinct that this is one of the key criterias used to distinguish between the two types of neurons (see Skottun et al., 1991).

Therefore, the response of units to gratings are plotted in a PSTH and a discrete fourier transform using a fast fourier transform is run on the resulting trace (using custom code in MATLAB; see appendix). The F0 component

thus obtained will equal the mathematical mean of the trace. The F1 component would be related to the temporal frequency of the stimulus. Since simple cells show half-wave rectification, the F1 component of the FFT is doubled and this is taken as the F1 component of the response. The modulation ratio will be calculated as calculated by Van Hooser et al., 2013 (for better comparability) and if it is greater than 1, then the unit is considered complex. If it is less than 1, then it is considered simple. The response magnitude will be used accordingly.

5.7.3 Measures of orientation tuning

Two separate measures of orientation tuning will be calculated; the orientation selectivity ratio, which gives information on the optimum and orthogonal orientations and the circular variance which gives an indication of the circularity of the responses of the neuron. The formulas for these are as shown below.

5.7.4 Spatial Frequency Tuning

Spatial frequency tuning curves were fit to the spatial frequency responses of a neuron. The SF tuning curve is ideally defined by a difference of Gaussian curve as specified in REFERENCE.

Chapter 6

**Where do orientation biases
come from?**

6.1 Abstract

Though theories of orientation selectivity suggest that orientation biases observed in V1 inputs are the result of excitatory convergence, studies have shown that bias in the inputs may be inherited from neurons in sub-cortical structures, especially the retina and the lateral geniculate nucleus (LGN). Congruent with this theory, retinal and LGN neurons have been shown to be tuned to orientation at higher spatial frequencies. If orientation selectivity arises from the retina, it should be evident in other targets of retinal projections. The superior colliculus (SC) is one such area. Here, I examined the orientation selectivity of SC neurons in tree shrews using thin bars and gratings of various spatial frequencies. I found that SC neurons show orientation tuning comparable to that observed in layer 4 of V1 in the tree shrews and orientation biases reported in the retina and the LGN of cats and macaques. This orientation selectivity was more evident at higher spatial frequencies. These results indicate that orientation tuning observed in the inputs to the cortex maybe generated from the orientation biases present in earlier visual areas.

6.2 Introduction

The theory of excitatory convergence (Hubel & Wiesel, 1962) suggests that orientation tuning in the primary visual cortex (V1) is derived from inputs from circular lateral geniculate nucleus (LGN) neurons that are arranged in a row converging on the V1 neuron. While this theory has garnered a lot of support, it has also been widely contested. In this chapter, I aim to examine one of the main assumptions of this theory: that subcortical neurons are unoriented.

A long list of studies have shown that orientation biases are present in subcortical structures. Levick and Thibos (1980) initially showed that retinal ganglion cells were tuned to orientation at higher spatial frequencies. These results have since been replicated in both cats and macaques at the level of the retina and the LGN. The retinal orientation biases are set to be derived from the natural growth pattern of the retina which elongates the dendritic fields. Given that orientation tuning is only observed at higher spatial frequencies and the fact that V1 neurons only respond at higher spatial frequencies, the degree of orientation tuning observed in the inputs to V1 can be generated by a mere sharpening of biased inputs.

Intracortical recordings in cat V1 show that the EPSPs observed in cortical neurons are tuned to orientation. Ferster (1986) argued that this orientation tuning may be explained by excitatory convergence. However, Pei et al (1994) showed that when the dynamics of orientation selectivity were

examined, the earlier EPSPs showed broader orientation tuning, similar to that reported in the LGN and retina. These broader signals were further tuned by inhibition observed as IPSPs. Both excitatory convergence and retinal orientation biases can explain orientation tuning of cortical inputs. However, only retinal bias model is consistent with the degree of orientation tuning of the inputs and the dynamics of the PSPs.

If the retina were the seed of orientation selectivity in the visual system, we should be able to detect orientation bias in parts of the brain that also receive inputs from the retina. The superior colliculus, which forms an alternate pathway to the visual cortex receives direct inputs from the retina. The superior colliculus neurons in cats and macaques however, prominently show no orientation biases. Recent studies have somewhat redeemed the SC, with rodent SC neurons showing sharp orientation tuning. While there seems to be a different model of orientation selectivity and cortical organisation in the rodent, I believe that SC neurons that receive direct retinal inputs will also be tuned to orientation. This is because orientation tuning in subcortical areas are only present at higher spatial frequencies and studies that looked for orientation tuning in the SC did not take this into account. Here I looked at orientation biases in the tree shrew superior colliculus.

The tree shrew was chosen for a few important reasons, foremost of which is that it has a large, distinctly laminated superior colliculus that has been well characterised. Studies showed that as in macaques and cats, the superficial layers of the shrew SC receives direct input from the retina and has been

implicated in form discrimination. These layers are also part of an independent pathway to the extrastriate cortex which is essential in form perception. However, unlike cats and macaques, in the tree shrew superior colliculus, a previous study showed that a small proportion of neurons in the superficial layers of the shrew SC had distinctly elongated fields. This study might have missed any small orientation biases as only fields that were 3 or more times longer than they were wide were classified as orientation selective.

Here I examined orientation biases in the SC neurons in attempt to show that orientation tuning in the inputs to the cortex was a reflection of the bias observed in the retina. We hypothesised that orientation tuning will be revealed in the superior colliculus at higher spatial frequencies. In particular:

- a) When using thin, moving bars, the neurons will be tuned to orientation and;
- b) When tested using gratings of different spatial frequencies and orientation, orientation tuning will be evident at higher spatial frequencies.

6.3 Methods

6.3.1 Electrophysiology

The superior colliculus in the tree shrew is large and well laminated structure and runs from the posterior edge of the brain to AP 2. Following surgery, a craniotomy was performed over the location of the superior colliculus. High impedance tungsten microelectrodes were lowered into the brain and the signal was amplified and filtered and fed into an audio speaker as well as an

analog to digital converter and recorded. The SC was identified by listening to the neuronal activity in the speaker. The data was recorded as a spike trace using the spike 2 software. The spikes were templated and the spike timing exported as a text file. Further analysis was performed using custom MATLAB code.

6.3.2 Stimuli

Stimuli was presented using a Barco monitor and the stimuli were generated using Visage (VSG). For each SC neuron, the preferred orientation was measured using a thin bar sweeping bi-directionally (Check if there is a particular size of the bar that we preferred). Then, the spatial frequency response to a gratings of different orientations was also measured.

6.3.3 Data Analysis

As mentioned in section 3 (Methods), Spike Density Functions were constructed for both the bar and gratings. For orientation tuning recorded using a bar, the maximum response for each orientation was plotted on a polar diagram. The circular mean of the angular response was considered the optimum orientation. The circular variance was calculated as a measure of sharpness of the orientation tuning.

For the gratings, the FFT of the spike density function was calculated. Then the F0/F1 ratio was calculated. If the ratio was less than 1, the cell

was deemed to be X- like and the F1 component of the response was used for further analysis. If the ratio was greater than 1, the cell was considered non-linear and the F0 component was used.

The bandwidth during which the superior colliculus neurons responded for the optimum orientation but not for the orthogonal orientation was calculated. In order to do this, a minimum response was first defined as the response rate at the spatial frequency where the response between the optimum and orthogonal orientations were not significantly different. The SF bandwidth was then the difference between the SF when the response for the orthogonal orientation reached the minimum response and the SF where the optimum orientation response reached the minimum response.

6.4 Results

6.4.1 Anatomical location of units

Using the histological reconstructions described in methods, the laminar position of 21 units from three Tree Shrews was determined. The results are presented in Figure 6.1. The reconstruction shows that most neurons were present in the Stratum Griseum Superficiale (SGS) where the majority of retinal inputs terminate.

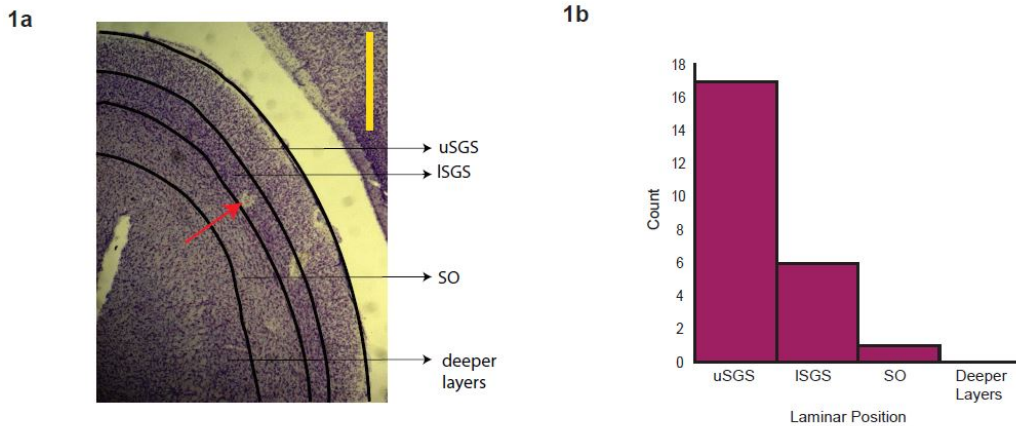


Figure 6.1: Histology. a) A section of tree shrew superior colliculus showing electrolytic lesions. Red arrow points to an electrolytic lesion. Scale bar (yellow vertical line) denotes 1000 m. b) A summary of laminar position of recorded units in the superior colliculus. Abbreviations: uSGS- upper Stratum Griseum Superficiale; ISGS- lower Stratum Griseum Superficiale; SO- Stratum Opticum.

6.4.2 Orientation Selectivity

The responses of a representative neuron to thin bars of changing orientation are presented in figure 6.2. The response shown in the figure is the average spike rate of the neuron over 10 trials. The corresponding orientation tuning curve along with the orientation tuning curves of our most and least tuned neurons are presented in the figure below.

The circular variance was calculated as described earlier to indicate the degree of orientation tuning demonstrated by the neurons studied. Any neuron that had a CV of greater than 0.9 was said to be non-oriented for the purposes of this study. The median CV we observed was 0.82 with a range of

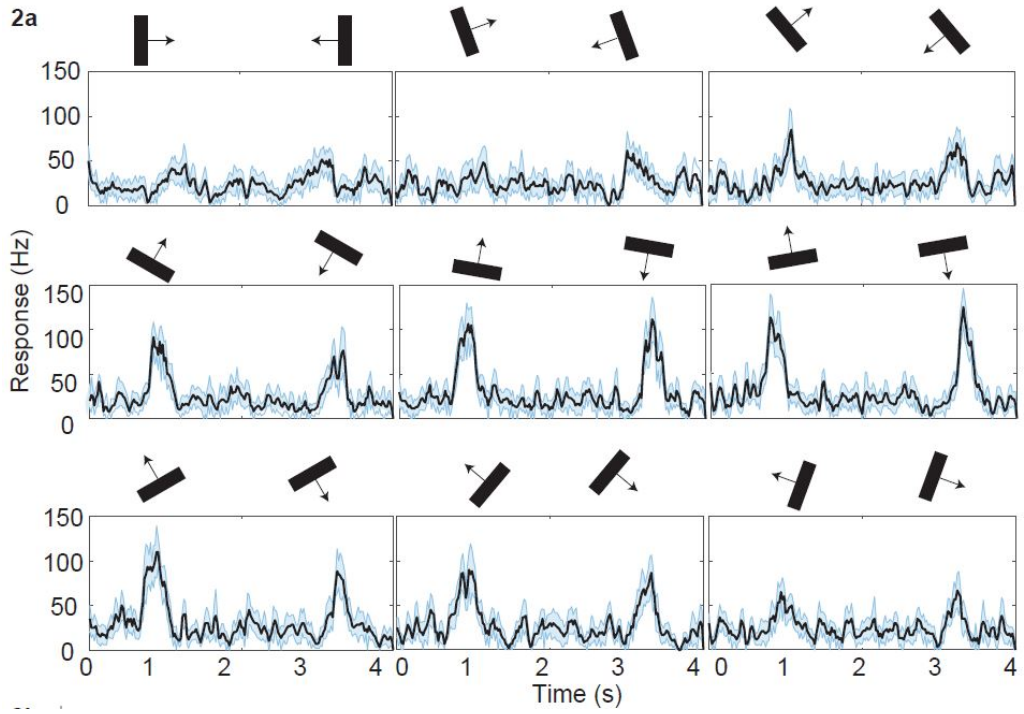


Figure 6.2: Orientation response of an example cell. 2a) Spike density functions (20 ms bins smoothed over 3 bins) of the neurons response to oriented bar (direction of motion above each peak).

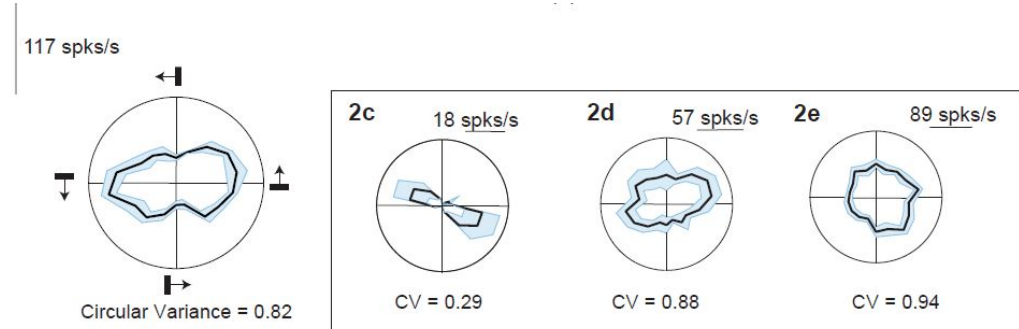


Figure 6.3: Polar plot showing the orientation tuning of the bar. Error bars denote Standard error. Orientation tuning curves of the sharpest (2c) and the least tuned (2d) neurons included in our analysis. (2e) was the least tuned neuron in our sample

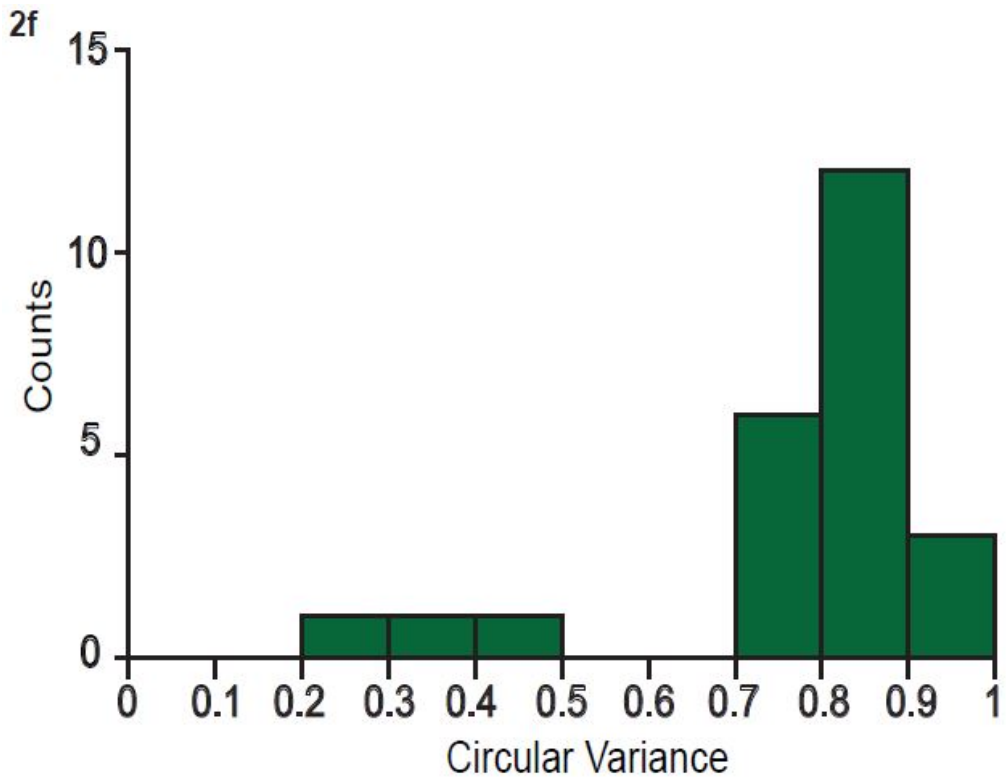


Figure 6.4: This figure demonstrates the distribution of circular variances of all neurons.

[0.21, 0.94]. Two neurons which had a CV of greater than 21 were excluded from further analysis. A distribution of the circular variances is presented below.

6.4.3 Spatial Frequency Tuning

The spatial frequency response of the neurons were also tested in relation to different orientations. The difference in response between the optimum and

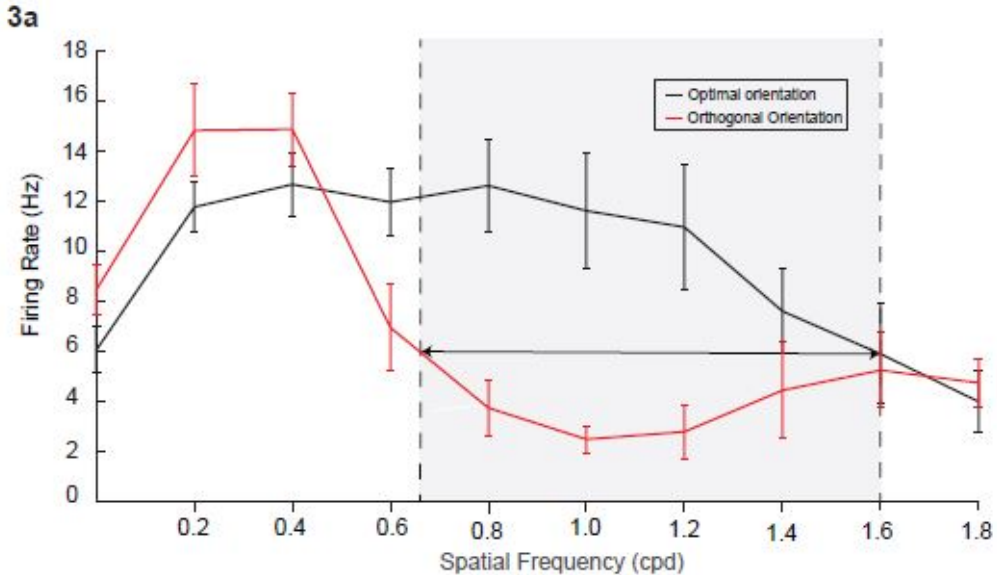


Figure 6.5: Example SF tuning curves for optimal and orthogonal orientations. The cut-off frequency at the optimal orientation is the SF at which the response at optimal orientation is no longer significantly different from the response at orthogonal orientation. The response at the cut-off frequency for optimum orientation is called the minimum response. For the orthogonal orientation, the cut-off frequency was the SF at which minimum response was first reached.

non-optimum orientation was calculated as described in the methods. We found that on average, the response to the orthogonal orientation reached the minimum 0.5 cpd before the response to the optimum orientation; with the 95 percent CT= [0.4, 0.6]]

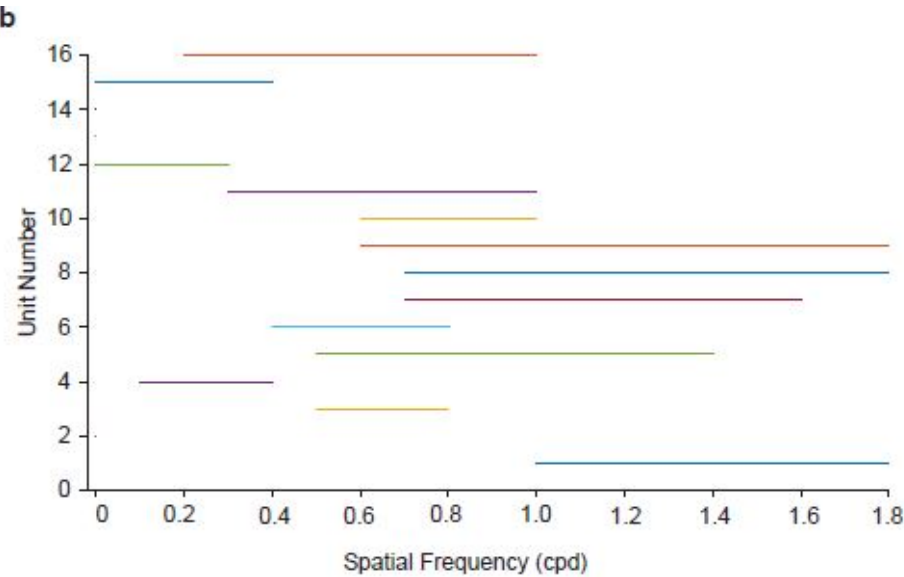


Figure 6.6: The difference between the cut-off frequencies for the optimum and orthogonal orientations for 16 units is shown in Figure 3b.

6.5 Discussion

Results show that superior colliculus neurons are tuned to orientation at higher spatial frequencies. I postulated that if the orientation tuning observed in the inputs to the cortex indeed originated in the retina rather than through the convergence of unbiased geniculate inputs, then if orientation tuning is measured along a pathway other than the geniculo-striate pathway, orientation biases similar to that observed in the retina would be found in the superior colliculus, which is in an alternative pathway. That is, when tested with thin bars, the SC neurons will be orientation selective and when tested with grating stimuli, the orientation tuning would be predominantly

observed at higher spatial frequencies. These findings are comparable to Our results are congruent with this finding suggesting that orientation tuning in the primary visual cortex originates from biases in the retina.

6.5.1 Anatomical Relevance

What did you find? Orientaiton bias in the superior colliculus at higher spatial frequencies. So what? well orientation bias is in the retina. Ok? And everyone thinks that orientation selectivity is generated in the cortex. So what does this show? It shows that orientation selectivity is present earlier in the visual system. Is this the first time that's been shown? No. It's been shown in the LGN and in the retina. OK? So what's new? Reporting orientation bias in the superior colliculus means that orientation bias is probably inherited from the retina. So what? Being present earlier in the visual system means that the visual system doesn't have to reinvent the wheel over and over again.

6.5.2 Orientation selectivity in shrew superior colliculus

6.5.3 Direction selectivity

6.5.4 Similarities and differences with other species

Chapter 7

**Orientation anisotropies in the
inputs to the primary visual
cortex of macaques**

7.1 Abstract

The first part of this thesis looked at how sharp orientation tuning may be generated from broadly oriented sub-cortical inputs. In this chapter, the role of subcortical inputs in generating cortical architecture is examined. While there are many theories that explain orientation selectivity and cortical architecture individually, there is no one theory that explains both phenomena. A recent theory attempts to explain both cortical architecture and orientation selectivity using previously presented evidence and also evidence presented previously in this thesis. First, and as shown in the two previous chapters, subcortical neurons are broadly tuned to orientation. This orientation bias is probably inherited from the orientation bias in the retina. Second, instead of all orientation being evenly distributed, certain orientation anisotropies have been demonstrated in every animal studied so far. He we posit that the cortical architecture is derived from broadly tuned inputs arriving in a limited number of orientations. Here, we used optical imaging of intrinsic signals to examine inputs to the cortex and found that these inputs are tuned to one predominant orientation; the radial orientation.

7.2 Introduction

- Summarise research on establishing cortical architecture. - Introduce the issue of a common unifying theory of both cortical architecture and orientation selectivity. - Explain briefly sagar's theory. - Reasons - Explain the experiment.

7.3 Methods

7.3.1 Data Collection

Optical Imaging of intrinsic signals

Optical imaging of intrinsic signals was used to obtain the haemodynamic change related to the response of neural response to orientation stimuli. The OI setup involved two camera lenses arranged in a tandem fashion connected to a CCD camera. The tandem lens arrangement allowed for a narrow plane of focus. An LED light source was used to illuminate the cortical surface. Before stimulus presentation, a high contrast, green image of the surface of the imaged cortex was obtained by illuminating the cortical surface with green light ($\lambda=545$ nm). This provided us with cortical landmarks which was later used in determining the locations for electrode tracks for topographical recordings. Following this, the plane of focus of the camera setup was changed to between 550-700 microns beneath the surface of the cortex and the wavelength of the illuminating light was changed to 630 nm.

18 frames, each 400 ms long was collected for each stimulus presentation. The signal to noise ratio was enhanced by acquiring data over 50 trials collected in 10 blocks of 5 trials each. Where possible, given the condition of the imaged area and the animal, the experiment was repeated a second time. Using the OI data acquisition system, each block was exported as a MATLAB file. Each individual frame in a block was the average of that frame for 5 trials. Analysis was conducted on the exported MATLAB files.

Stimulus

Visual stimuli were generated by a Visage stimulus generator (SDL, Cambridge Research Systems, UK) at 80 Hz on a BARCO monitor (Reference Calibrator plus; Barco Video and Communications, Belgium) at 57 cm from the animal. Stimuli were full-field, high contrast, square-wave gratings (1-4 cycles/deg moving at 1-1.5Hz) and presented in 8 different orientations drifting in one direction and then the other. Each grating stimulus was presented for 7.2 s with an interstimulus interval of 10s between gratings when the animal viewed a blank screen. Data was collected for 50 complete presentations of each stimulus.

Topographical recordings

The study of radial bias requires the careful plotting of receptive field locations in relation to their cortical location. In order to obtain this, we used high impedance tungsten microelectrodes (12 M Ω) to record from pre-

determined locations on the imaged cortical surface. The signal was passed through an amplifier with x 10,000 times gain and filtered between 300 and 3000 Hz. The filtered signal was then visualised on an oscilloscope and fed through an audio speaker to aid us in plotting the receptive fields. We first plotted the location of the fovea (if visible) and the optic nerve with blood vessel markers using a fundus camera. We then carefully hand plotted the location of the receptive fields using handheld stimuli from the corners of the imaged area. In between each electrode penetration, where possible, we also replotted the location of the fovea and optic nerve head in order to account for eye movement.

7.3.2 Analysis

Image Analysis

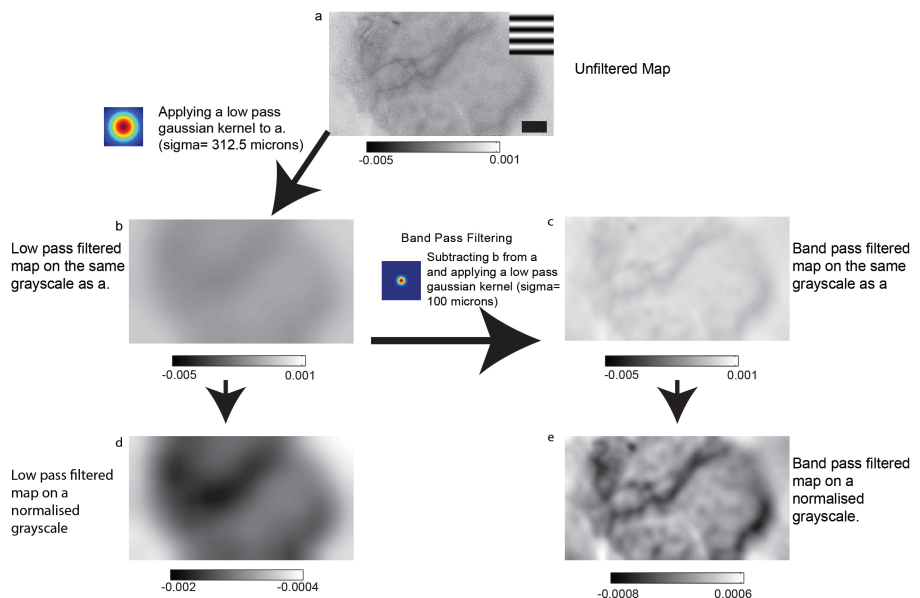
We analysed the images obtained using optical imaging of intrinsic signals as follows. During data collection, we collected 18 frames per condition in each of 50 trials. These were organised as 5 trials in 10 blocks. Of the 18 frames collected, we took the mean of frames 3-16 (14 frames) and subtracted the first frame from the averaged frames for each block. The mean of 10 blocks was calculated. This gave us the unfiltered single condition maps (referred to as veridical SCMs). Traditionally, when analysing the images obtained using optical imaging of intrinsic signals, the following method is used. The veridical SCMs are band pass filtered using the method described in figure

4.1. The unfiltered map is first low pass filtered using a large filter. Here we have set a value of 312.5 microns on a gaussian filter. This removes the low frequency information. By subtracting the low pass image from the original image, we preserve only the high spatial frequency information. This will be called the high-pass single condition map. The high pass image is then smoothed with a gaussian filter with a smaller sigma value (100 microns). This is the band pass filtered single condition map or more commonly just referred to as the single condition map. The single condition maps are then vector averaged to look at the angular mean of individual pixels. This will produce the traditional filtered orientation tuning maps. In our study, we also vector averaged the veridical SCMs. We called the maps derived this way the veridical single condition maps.

Analysis of electrophysiological recordings

In order to determine the azimuth and elevation of receptive fields obtained during the experiment, we set the co-ordinates of the fovea at (0,0). We obtained the azimuth and elevation of receptive fields in relation to the centre. If there were eye movements during the experiment, (0,0) was assigned to the new foveal location. Receptive field locations were determined in relation to foveal locations plotted closest to the recording in order to get as accurate a receptive field location as possible.

Using the receptive field locations thus calculated, we used the eccentricity, azimuth and elevation values to calculate iso azimuthal and iso elevation



Supp Fig1: Filtering process: a) An example of an unfiltered single condition map. Inset is the stimulus condition. b) SCM after applying low pass filter ($\sigma = 625$ microns). Map b is subtracted from map a and a low pass filter ($\sigma = 100$ microns) is applied to the resulting map to give the band-pass filtered map in c. The maps b and c have the same gray scale as the unfiltered map in a, showing absolute intensity values. The maps in d and e are the same maps in b and c, respectively normalised to their minimum and maximum values , as it is usually done in most studies. Scale bar is 1mm.

Figure 7.1: Method Figure

lines on the cortex. We used the magnification factor calculations in the macaque cortex published by Dow et al to calculate the inverse magnification factor; How far one needs to move on the cortex to traverse 1 degree in visual space, given the eccentricity of the receptive fields. The formula had a resolution of 10 minutes of visual space. We used these values to calculate the iso-azimuthal and iso- elevation lines.

Comparing the radial angle of the receptive field to the optimum orientation of orientation maps

We compared the radial angle of the receptive to the optimum orientation obtained on the orientation maps on two spatial scales - ROI and single pixel level. An ROI or region of interest was determined as follows. Using the magnification factor calculation as described above, we determined the receptive field location of points on the cortex spaced 375 microns (15 pixels) apart. These points formed the centre of the ROIs and their receptive field location was used to determine the radial angle of the ROI. The optimum orientation was obtained by calculating the mean orientation of 750 micron² area around the centres of the ROI from the filtered and the unfiltered maps. The absolute difference between the radial orientation of the centre of the ROI and the optimum orientation of each ROI was calculated. A histogram was of the absolute differences was calculated and the differences were grouped in 22.5 degree steps. The bin width of 22.5 degrees was chosen because the stimulus orientation changed in 22.5 degree step and we believed that differences

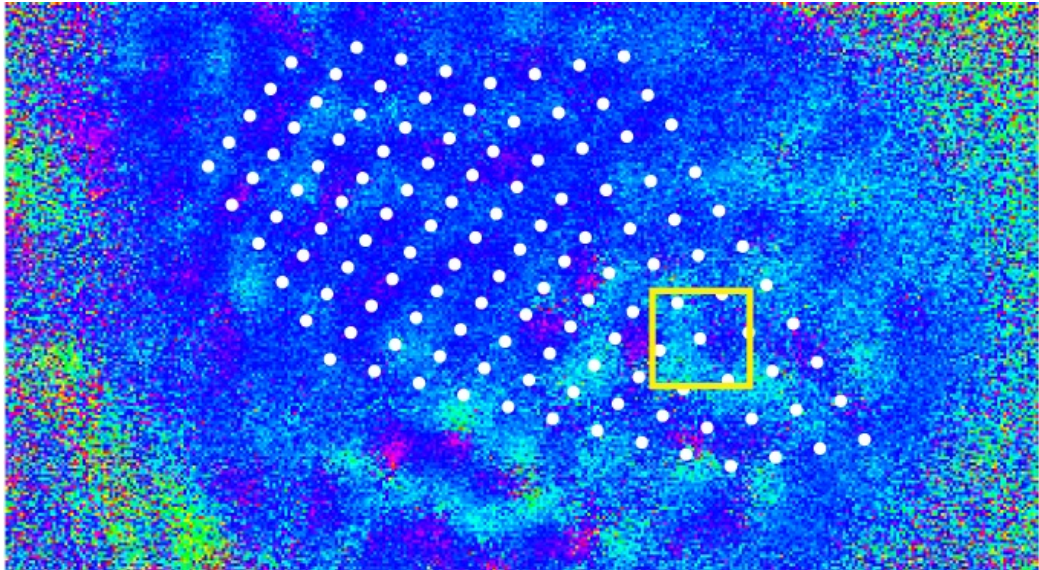


Figure 7.2: Method Figure for ROI

smaller than this may not mean much. We also calculated the difference between the mean radial orientation and the optimum orientation of all the pixels within the analysed area in order to not smooth over any smaller scale differences which may otherwise be smoothed. The differences of the single pixels were also grouped in 22.5 degree bins with the radial orientation set as 0 degree. This was repeated across all animals and the group data are presented in the results. See methods figure 2 for more information on how the maps were calculated. We restricted the area we imaged to show a relatively flat area of the cortex. Any ROIs and pixels outside this area were ignored. See figure 2. We also grouped the histograms of the ROI and the single pixels according to their optimum orientation to see if there were any other orientation biases we may have missed otherwise.

Investigating for the presence of cardinal orientation biases in the inputs

In the above method, the orientation values of the single pixels was determined using the angular mean of that pixel obtained by vector averaging the single condition maps. We also used another method where we grouped the pixels according to the orientation to which they gave the maximum response in the single condition maps. This gives the added bonus of not smoothing over any small anisotropies in the response of a pixel. These results are presented in figure number.

7.4 Results

Examining Single Condition Maps

Orientation Tuning Maps

Group Data based on ROIs

Group Data based on Single pixels

Accounting for sample size

Examining inputs

Accounting for sample size

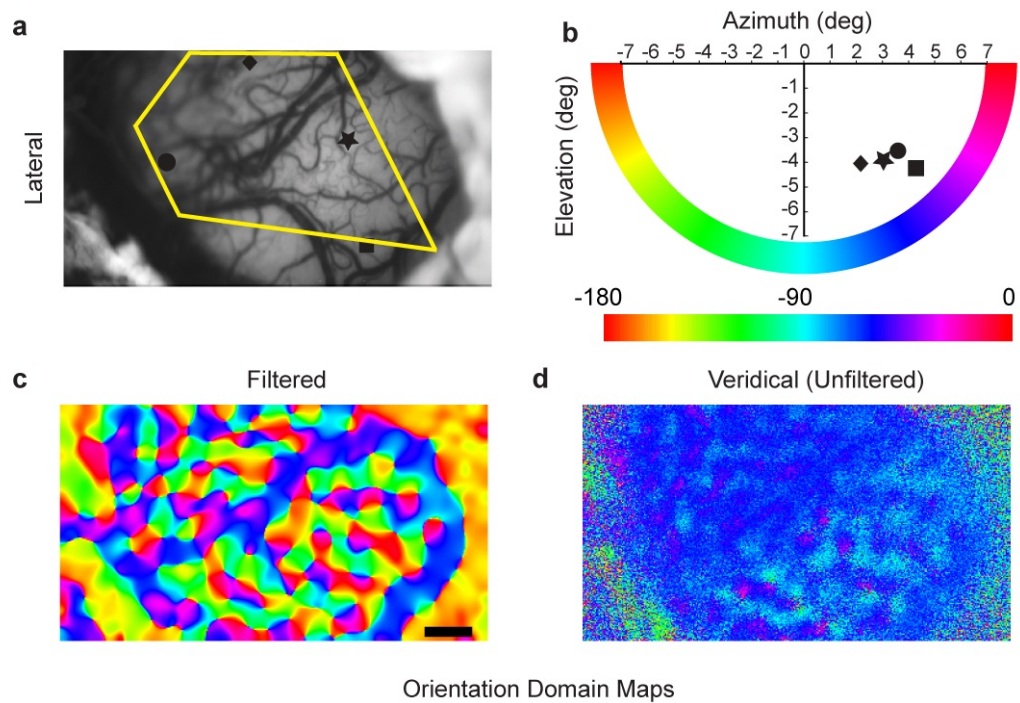


Figure 7.3: Figure 1

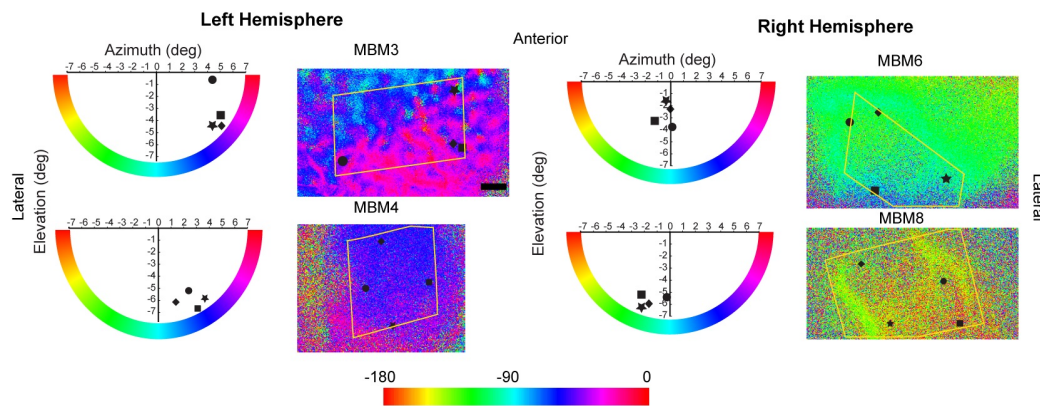


Figure 7.4: Figure 2

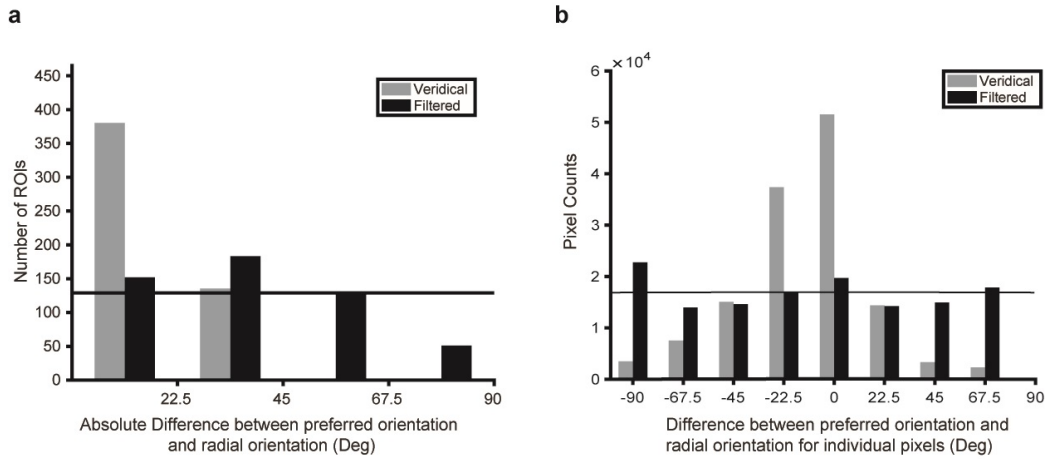


Figure 7.5: Figure 3

7.5 Discussion

7.6 Conclusions

Chapter 8

Issues to be solved

- The issue of linearity: Work on this. There is F0 and F1. F0 is the non-linear component. F1 is linear (in very simple terms.) - So depending on the process we are looking at, we would have to figure out what the response is.
- But orientation tuning has both linear and non linear processes. - Tasks for the next couple of days: linear and non linear processes in orientation tuning. This will help us define what responses we are looking at.